

# Conformations of Banana-Shaped Molecules Studied by $^2\text{H}$ NMR Spectroscopy in Liquid Crystalline Solvents

Lucia Calucci,<sup>†</sup> Claudia Forte,<sup>\*,†</sup> Katalin Fodor Csorba,<sup>‡</sup> Benedetta Mennucci,<sup>§</sup> and Silvia Pizzanelli<sup>†</sup>

*Istituto per i Processi Chimico Fisici, CNR, Area della Ricerca di Pisa, via G. Moruzzi 1, 56124, Pisa, Italy, Research Institute for Solid State Physics and Optics, Hungarian Academy of Sciences, Budapest, Hungary, and Dipartimento di Chimica e Chimica Industriale, Università degli Studi di Pisa, via Risorgimento 35, 56126, Pisa, Italy*

Received: September 15, 2006

CIPbis11BB and Pbis11BB, two banana-shaped mesogens differing by a chlorine substituent on the central phenyl ring, show a nematic and a  $B_2$  phase, respectively. To obtain information on the structural features responsible for their different mesomorphic behavior, a study of the preferred conformations of these mesogens has been performed by NMR spectroscopy in two nematic media (Phase IV and ZLI1167), which should mimic the environment of the molecules in their own mesophases, avoiding problems of sample alignment by a magnetic field. To this aim,  $^2\text{H}$  NMR experiments have been performed on selectively deuterated isotopomers of CIPbis11BB and Pbis11BB and of two parent molecules, CIPbisB and PbisB, assumed as models in previous theoretical and experimental conformational studies. We found that only a limited number of conformations is compatible with experimental data, often very different from those inferred from theoretical calculations in vacuo, indicating a strong influence of the liquid crystalline environment on molecular conformation. No significant differences between chlorinated and non-chlorinated molecules were found, this suggesting that chlorine does not change the molecular conformational equilibrium, as previously proposed.

## Introduction

In recent years, liquid crystalline phases formed by bent core molecules have been the subject of many theoretical and experimental investigations.<sup>1,2</sup> It has been shown that these molecules, usually referred to as banana-shaped, can pack to form nematic and smectic phases, typical of calamitic mesogens, but they can also organize into novel types of lamellar or columnar liquid crystalline phases, called B phases. Up to now, seven B phases with different structures have been reported in the literature, some of them showing polar order within the layers or the columns resulting in peculiar electro-optical properties of interest for technological applications.<sup>2</sup> In view of these properties, many efforts have been made for elucidating the relationships between the chemical structure of banana-shaped mesogens and their mesomorphic behavior.<sup>1,3–6</sup> The influence of different structural elements (molecular size, bend angle, substituents and linking groups, length, and polarity of the terminal chains) on the phase structure and transition temperatures has been studied on five ring core molecules. In particular, it has been shown that the introduction of one or two chlorine atoms into a central 1,3-phenylene ring, the most common central ring in banana-shaped liquid crystals, can determine the formation of a nematic phase instead of a B phase.<sup>1,7–9</sup> It has been argued that the presence of chlorine alters the conformational equilibrium of the molecule, which therefore assumes a nearly rod-like shape and packs preferentially in a

nematic phase. However, differences in the dipole moments could also be seen as an indication of the different mesomorphic behavior.<sup>10</sup>

In this work, we focused on the two banana-shaped mesogens shown in Figure 1, CIPbis11BB and Pbis11BB, exhibiting a nematic and a  $B_2$  phase, respectively,<sup>9</sup> with the aim of understanding which structural features determine the different mesomorphism of these compounds. To this purpose, experimental techniques and theoretical calculations have been previously applied to these systems. In particular, in an NMR study on CIPbis11BB in the nematic phase, values of the bending angle, defined as the angle between the para axes of the intermediate phenyl rings, of  $144.3^\circ$  and  $136.6^\circ$  were derived from  $^2\text{H}$  and  $^{13}\text{C}$  data, respectively.<sup>11</sup> However, many crude assumptions were made to extract information from experimental data; for example, a unique molecular principal axis located in the plane of the central ring was used to describe the orientational order, and orientation and principal values of  $^{13}\text{C}$  chemical shift tensors were not directly determined but assumed to be equal to those of model compounds. Moreover, no analogous experiments could be performed on Pbis11BB in the  $B_2$  phase due to difficulties in sample alignment,<sup>12</sup> and therefore comparison between the two mesogens in their own liquid crystalline phases was not possible. Both semiempirical<sup>9</sup> and DFT<sup>13</sup> calculations were performed to supply for the lack of experimental information. The results indicated that twisted conformations are energetically favored for both CIPbis11BB and Pbis11BB; however, strong differences were observed in the energy barriers that are lower than 0.7 kcal/mol for the non-chlorinated molecule and about 10 kcal/mol for the chlorinated one. The different conformational equilibria for the two molecules result in a larger bending angle for CIPbis11BB, even

\* Corresponding author. E-mail: c.forte@ipcf.cnr.it; phone: +39-050-3152462.

<sup>†</sup> Istituto per i Processi Chimico Fisici.

<sup>‡</sup> Hungarian Academy of Sciences.

<sup>§</sup> Università degli Studi di Pisa.

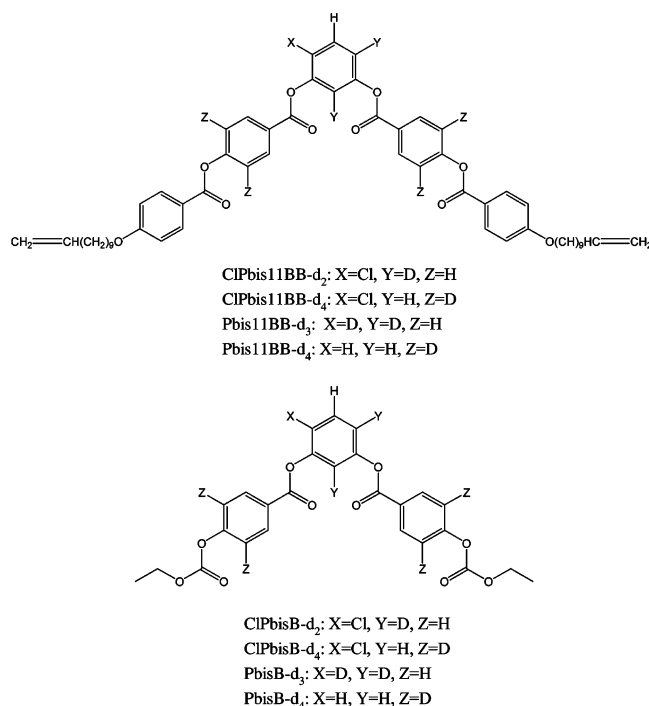


**Figure 1.** Molecular structure and deuteration of Pbis11BB, CIPbis11BB, PbisB, and CIPbisB.

if it is still lower than 130°, which has been indicated as the maximum limiting value for the bending angle in banana mesogens displaying a B<sub>2</sub> phase.<sup>13</sup> However, it must be pointed out that the results strongly depend on the theoretical method used in the calculation and, most importantly, refer to the molecule in vacuo, excluding the influence of intermolecular forces on the conformation, which, instead, has been found to be very important for banana-shaped molecules.<sup>7</sup>

In this context, we decided to investigate molecular conformations of CIPbis11BB and Pbis11BB by NMR in liquid crystalline solvents that should mimic the environment of the molecules in their own mesophases and allow easy alignment of the sample, particularly important for Pbis11BB, which is very difficult to align in its B<sub>2</sub> phase.<sup>12</sup> <sup>2</sup>H NMR experiments were performed at different temperatures on selectively deuterated isotopomers of CIPbis11BB and Pbis11BB (Figure 1) dissolved in two nematic mixtures differing in the sign of the diamagnetic susceptibility anisotropy, Phase IV and ZLI1167. The two solvents were chosen to exclude specific solute–solvent interactions, possibly biasing the conformational equilibrium.

The same experiments were performed also on the three ring molecules CIPbisB and PbisB (Figure 1) with the aim of verifying if these simpler molecules can be suitably used as models for the corresponding five ring banana-shaped mesogens, as has been done in theoretical conformational studies.<sup>13–15</sup>

## Experimental Procedures

**Synthesis.** Synthetic pathways for the preparation of CIPbisB-*d*<sub>2</sub> (**3a**), PbisB-*d*<sub>3</sub> (**3b**), CIPbis11BB-*d*<sub>2</sub> (**6a**), Pbis11BB-*d*<sub>3</sub> (**6b**), CIPbisB-*d*<sub>4</sub> (**3c**), PbisB-*d*<sub>4</sub> (**3d**), CIPbis11BB-*d*<sub>4</sub> (**6c**), and Pbis11BB-*d*<sub>4</sub> (**6d**) are reported in Scheme 1.

4-(Ethoxycarbonyloxy)benzoyl chloride (**1a**) and its isotopomer **1b** were prepared according to the procedure reported in ref 16. 4-Chloro-resorcinol (**2c**) and resorcinol (**2d**) were purchased from Aldrich and used without further purification. 4-(10-Undecenyoxy)benzoyl chloride (**5**) was prepared according to the procedure reported in ref 17.

**4-Chloro-resorcinol-*d*<sub>2</sub> (**2a**).** 4-Chloro-resorcinol (5.00 g, 34.6 mmol), D<sub>2</sub>O (15 mL), and a catalytic amount of D<sub>2</sub>SO<sub>4</sub> (0.5 mL) were placed in an autoclave and heated at 160 °C for 18 h. After cooling to room temperature, the mixture was extracted with chloroform (30 mL). The organic phase was washed with 5% sodium carbonate until it became neutral and dried over magnesium sulfate, and the solvent was evaporated yielding **2a** (3.80 g, 74%).

**Resorcinol-*d*<sub>3</sub> (**2b**).** Resorcinol (10.00 g, 90.9 mmol) was dissolved in D<sub>2</sub>O (15 mL), and D<sub>2</sub>SO<sub>4</sub> (0.5 mL) was added as a catalyst. The reaction mixture was refluxed in argon atmosphere for 30 h. After extraction with ethyl acetate, the organic phase was washed with water (10 mL) and dried on magnesium sulfate, and the solvent was evaporated. The solid material obtained was washed with petroleum ether, and 8.33 g of **2b** (83%) were collected.

**4-Chloro-1,3-phenylene Bis(4-ethoxycarbonyloxy)benzoate-*d*<sub>2</sub> (**3a**).** 4-(Ethoxycarbonyloxy)benzoyl chloride (**1a**) (4.00 g, 17.5 mmol) was reacted with 4-chloro-resorcinol-*d*<sub>2</sub> (**2a**) (1.26 g, 8.7 mmol) in dry 2-butanone in the presence of triethyl amine (2.5 mL, 25.0 mmol). After stirring at room temperature for 2 days, the solvent was evaporated. After treatment with 1,2-dichloroethane, the crystals formed were filtered off. Then, the solid residue was crystallized from chloroform–petroleum ether to yield **3a** (4.34 g, 93%).

**1,3-Phenylene Bis(4-ethoxycarbonyloxy)benzoate-*d*<sub>3</sub> (**3b**).** 4-(Ethoxycarbonyloxy)benzoic acid chloride (**1a**) (4.00 g, 17.5 mmol) and resorcinol-*d*<sub>3</sub> (**2b**) (1.00 g, 8.7 mmol) were reacted in dry 2-butanone (25 mL) in the presence of triethyl amine (2.2 mL). After stirring at room temperature for 2 days, the solvent was evaporated, and the solid material was treated with 10 mL of D<sub>2</sub>O. After filtration, the residue was dried and crystallized consecutively from ethyl acetate, chloroform–petroleum ether, and ethanol to yield **3b** (4.30 g, 90%).

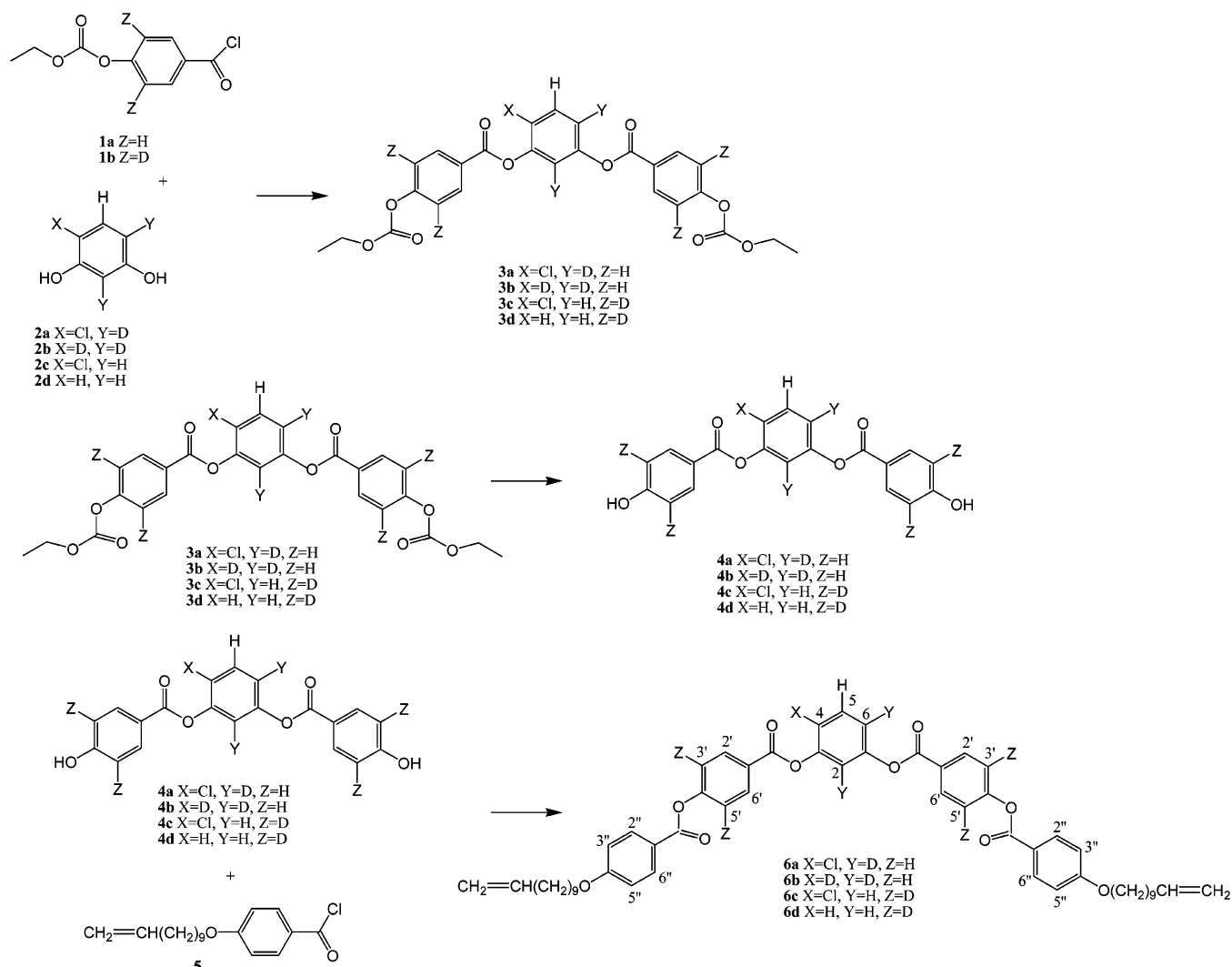
**4-Chloro-1,3-phenylene Bis(4-hydroxy)benzoate-*d*<sub>2</sub> (**4a**).** 4-Chloro-1,3-phenylene bis(4-ethoxycarbonyloxy)benzoate-*d*<sub>2</sub> (**3a**) (3.50 g, 7.0 mmol) was dissolved in dioxane (50 mL), cooled at 0 °C, and saturated with dry ammonia gas. Then, the cooling bath was removed, and the reaction was followed by TLC on Kieselgel 60 F<sub>254</sub> eluted with 1,2-dichloroethane. After about 30 min, the reaction mixture was cooled again to 0 °C and acidified with 20% hydrochloric acid. After extraction with benzene (50 mL), the organic layer was dried over magnesium sulfate, and the solvent was evaporated. Then, the solid material was crystallized from ethanol and D<sub>2</sub>O, thus obtaining 0.95 g (53%) of **4a**.

**1,3-Phenylene Bis(4-hydroxy)benzoate-*d*<sub>3</sub> (**4b**).** The procedure used to synthesize **4b** was the same as that reported for **4a**, except for the starting isotopomers.

**4-Chloro-1,3-phenylene Bis{4-[4'-(10-undecenyoxy)-benzoyloxy]}benzoate-*d*<sub>2</sub> (**6a**).** 4-(10-Undecenyoxy)benzoyl chloride (**5**) (1.00 g, 2.6 mmol) was reacted with 4-chloro-1,3-phenylene bis(4-hydroxy)benzoate-*d*<sub>3</sub> (**4a**) (0.50 g, 1.3 mmol) in the presence of triethylamine (0.5 mL) in 2-butanone at room temperature for 2 days. The reaction mixture was extracted with water (3 × 20 mL) and dried over magnesium sulfate, and then the solvent was evaporated. The crude product was purified by flash chromatography on a Kieselgel 60 (0.063–0.02 mm) column eluted with 1,2-dichloroethane. After evaporation of the solvent, 0.83 g (34%) of **6a** were obtained.

**1,3-Phenylene Bis{4-[4'-(10-undecenyoxy)benzoyloxy]}benzoate-*d*<sub>3</sub> (**6b**).** Compound **6b** was prepared starting from 1,3-phenylene bis(4-hydroxy)benzoate-*d*<sub>3</sub> (**4b**) and 4-(10-undecenyoxy)benzoyl chloride (**5**) according to the procedure

## SCHEME 1



described previously for **6a**. The reaction mixture was extracted with water ( $3 \times 20$  mL), dried over magnesium sulfate, and evaporated to dryness. The crude product was purified by flash chromatography on a Kieselgel 60 (0.063–0.02 mm) column eluted with 1,2-dichloroethane. After evaporation of the solvent, 0.39 g (34%) of **6b** were obtained.

**4-Chloro-1,3-phenylene Bis(4-ethoxycarbonyloxy)benzoate- $d_4$  (3c).** The procedure used to synthesize **3c** was the same as that reported for **3a** except for the starting isotopomers.

**1,3-Phenylene Bis(4-ethoxycarbonyloxy)benzoate- $d_4$  (3d).** The procedure used to synthesize **3d** was the same as that reported for **3b** except for the starting isotopomers.

**4-Chloro-1,3-phenylene Bis(4-hydroxy)benzoate- $d_4$  (4c).** The procedure used to synthesize **4c** was the same as that reported for **4a** except for the starting isotopomers.

**1,3-Phenylene Bis(4-hydroxy)benzoate- $d_4$  (4d).** The procedure used to synthesize **4d** was the same as that reported for **4b**, except for the starting isotopomers.

**4-Chloro-1,3-phenylene Bis[4-[4'-(10-undecenyloxy)benzoyloxy]]benzoate- $d_4$  (6c).** The procedure used to synthesize **6c** was the same as that reported for **6a**, except for the starting isotopomers.

**1,3-Phenylene Bis[4-[4'-(10-undecenyloxy)benzoyloxy]]benzoate- $d_4$  (6d).** The procedure used to synthesize **6d** was the same as that reported for **6b**, except for the starting isotopomers.

**$^2\text{H}$  NMR Experiments.**  $^2\text{H}$  NMR experiments were carried out on a Bruker AMX-300 WB, equipped with a 5 mm reverse

probe. The quadrupolar echo pulse sequence was employed with a  $\pi/2$  pulse of  $9.5 \mu\text{s}$  and a time interval between the two  $\pi/2$  pulses of  $35 \mu\text{s}$ . A total of 4000–16000 scans was acquired depending on the sample, with a recycle time of 1 s. Experiments were performed on solutions of the following four mixtures in the nematic solvent Phase IV (Merck, Darmstadt, mesophase range 289–349 K,  $\Delta\chi > 0$ ) and ZLI1167 (Merck, Darmstadt, mesophase range 305–356 K,  $\Delta\chi < 0$ ): (I) PbisB- $d_3$  and PbisB- $d_4$ ; (II) CIPbisB- $d_2$  and CIPbisB- $d_4$ ; (III) Pbis11BB- $d_3$  and Pbis11BB- $d_4$ ; and (IV) CIPbis11BB- $d_2$  and CIPbis11BB- $d_4$ . Concentrations were about 4 wt %. Measurements were performed at different temperatures throughout the solvent nematic range on cooling from the isotropic phase. The sample temperature was controlled employing a BVT 1000 (Eurotherm) variable-temperature unit, with a temperature stability of  $\pm 0.1$  K. The degree of deuteration and the position of the  $^2\text{H}$  nuclei were obtained from  $^1\text{H}$  NMR measurements in solution (see Supporting Information).

**Data Analysis.** Geometry optimizations were performed by the *Gaussian 03* package<sup>18</sup> using the B3LYP density functional method.<sup>19</sup> The basis set used was 6-31G for carbon, oxygen, and hydrogen atoms and LANL2DZ for chlorine atoms.

A global nonlinear least-squares fitting procedure was applied to the set of quadrupolar and dipolar couplings measured for each sample at all investigated temperatures by using a homemade Fortran program.

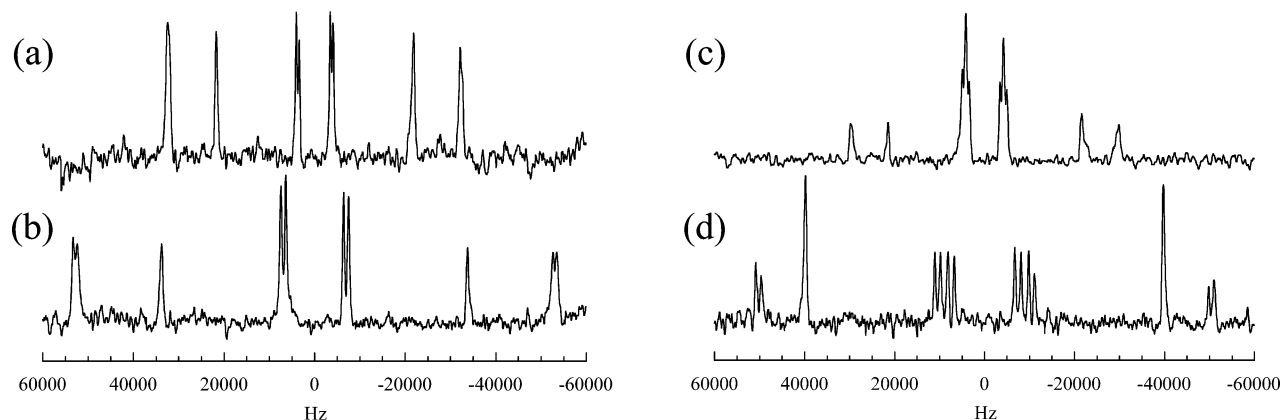


**Figure 2.**  $^2\text{H}$  NMR spectra recorded at  $T_{\text{NI}} - T = 20$  K of mixtures of the isotopomers Pbis11BB- $d_3$  and Pbis11BB- $d_4$  in (a) ZLI1167 and (b) Phase IV and of the isotopomers ClPbis11BB- $d_2$  and ClPbis11BB- $d_4$  in (c) ZLI1167 and (d) Phase IV.

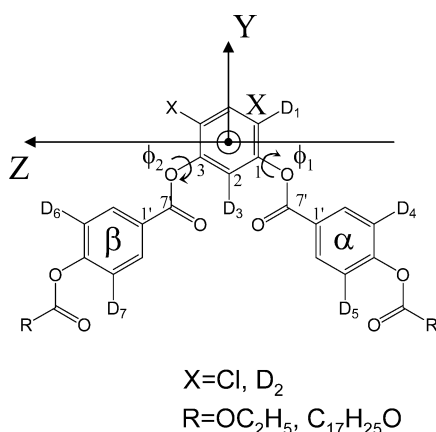


**Figure 3.** Molecular reference frame used in the data analysis. The dihedral angles are defined according to the convention proposed by Klyne and Prelog.<sup>25</sup>

## Results and Discussion

**$^2\text{H}$  NMR Spectra.**  $^2\text{H}$  NMR spectra were recorded on liquid crystalline solutions of selectively deuterated PbisB, ClPbisB, Pbis11BB, and ClPbis11BB in both Phase IV and ZLI1167, at different temperatures throughout the solvent mesophases. For each molecule, measurements were performed on mixtures of the isotopomers deuterated on the central and on the outer phenyl rings, as shown in Figure 1. A selection of representative spectra is reported in Figure 2. As can be observed, ClPbis11BB shows four quadrupolar doublets ascribable to  $D_1$ ,  $D_3$ ,  $D_{4,5}$ , and  $D_{6,7}$  (see Figure 3), considering that the lateral deuterated aromatic rings  $\alpha$  and  $\beta$  are not equivalent but the deuteria on the same ring are made equivalent by fast ring flip. Whereas the deuteria on lateral rings show splittings similar to those observed in the nematic phase of ClPbis11BB,<sup>11</sup> the two nonequivalent deuteria on the central ring do not show coincident splittings, and their values are sensibly higher than the single value observed in the pure nematic phase.<sup>11</sup> Pbis11BB shows only three quadrupolar doublets, indicating the equivalence of rings  $\alpha$  and  $\beta$  and therefore a  $C_2$  or  $C_s$  molecular symmetry. ClPbisB and PbisB show  $^2\text{H}$  NMR spectra analogous to those of the corresponding five ring mesogens, only with smaller splittings.

Considering that the principal order axis lies presumably close to the long molecular axis and assuming that the solutes follow the alignment of the solvent with respect to the magnetic field, the largest quadrupolar splitting can be assigned to  $D_1$  (equivalent to  $D_2$  in the case of the non-chlorinated molecules), whereas the smallest one(s) are due to deuteria on the  $\alpha$  and  $\beta$  rings. The assignment was confirmed by experiments on separate

solutions of the different isotopomers. In the case of the chlorinated molecules, the two smallest splittings could not be ascribed unequivocally to either  $D_{4,5}$  or  $D_{6,7}$ , so in the data analysis that follows, both assignments were considered.

At most two and three H–D dipolar doublets due to deuteria having protons in ortho position should be observable for the non-chlorinated and chlorinated molecules, respectively; however, poor spectral resolution or signal overlap prevented the measurement of the H– $D_1$  splitting at all temperatures.

The absolute values of the quadrupolar and dipolar splittings regularly increase with decreasing the temperature within the solvent mesophases. As can be seen in Figure 2, splittings in ZLI1167 are about half the corresponding ones in Phase IV, due to the different sign of  $\Delta\chi$  and consequently different alignment of the phase director, which is parallel and perpendicular to the magnetic field for Phase IV and ZLI1167, respectively.

**Data Analysis.** Quadrupolar and dipolar splittings measured from  $^2\text{H}$  NMR spectra in liquid crystalline phases can be expressed in terms of local order parameters by the following equations:

$$\Delta\nu_q = \frac{3}{2}qS_{\text{CD}} \quad (1a)$$

$$\Delta D_{\text{DH}} = -2K_{\text{DH}} \frac{S_{\text{DH}}}{r_{\text{DH}}^3} \quad (1b)$$

where  $S_{\text{CD}}$  and  $S_{\text{DH}}$  are the order parameters relative to the C–D and D–H vectors, respectively;  $q$  is the quadrupolar coupling constant, typically 185 kHz for aromatic deuteria;  $r_{\text{DH}}$  is the internuclear D–H distance, here fixed to the value of 2.49 Å; and  $K_{\text{DH}} = \gamma_{\text{D}}\gamma_{\text{H}}h/4\pi^2$ .

Transformation from a local reference frame to a molecular fixed frame requires the knowledge of geometrical parameters and, in the presence of internal motions, of the orientational–conformational distribution. For each conformer, the order parameters relative to the local frame ( $\alpha, \beta, \gamma$ ) can be expressed in a molecular fixed frame ( $X, Y, Z$ ) as

$$S_{\alpha\beta} = \sum_{ij} l_{\alpha i} S_{ij} l_{j\beta} \quad (2)$$

where  $l_{\alpha i}$  is the direction cosine between the  $\alpha$  and the  $i$  axes.

It must be pointed out that, in general, the orientational order of each conformer is described by an individual Saupe order matrix in the ( $X, Y, Z$ ) axes system, so that, if several conformers



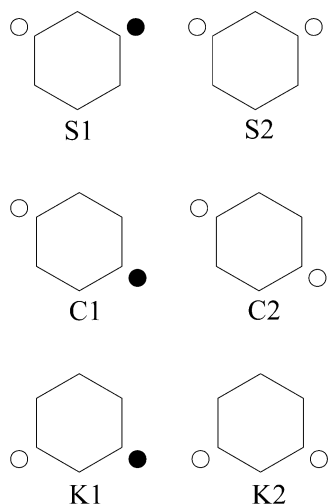


**Figure 4.** Schematic representation of possible conformers following ref 13. The hexagon represents the central phenyl ring, while the circles model the carboxylic  $\text{sp}^2$  oxygen atoms adjacent to it. The circle position up (i.e., both circles in S1 and S2) represents conformers characterized by corresponding  $\phi_i$  values greater than  $90^\circ$  but lower than  $270^\circ$ , while the position down (i.e., both circles in K1 and K2) represents conformers with  $\phi_i$  values in the ranges  $0^\circ$ – $90^\circ$  or  $270^\circ$ – $360^\circ$ . A CO group pointing above ( $\phi_i$  in the range  $0^\circ$ – $180^\circ$ ) or below ( $\phi_i$  in the range  $180^\circ$ – $360^\circ$ ) the plane of the central ring is represented by the symbol  $\circ$  or  $\bullet$ , respectively. When the two CO groups are on opposite sides with respect to the central ring plane, the conformers are defined as type 1, whereas when they are on the same side, they are type 2.

coexist, the local order parameters are weighted averages over the different conformers. Therefore, the local order parameters, and consequently the measured quadrupolar and dipolar splittings, depend on the geometry and order of the different conformers, as well as on their relative populations. This considered, the number of variables involved can be quite high (i.e., for  $N$  conformers up to  $5N$  Saupe order matrix elements and  $(N - 1)$  relative populations, in addition to geometric parameters). If, on one hand, geometric parameters, such as bond lengths and angles, can be determined from other techniques or calculated, no information is usually available independently on the number, population, and order parameters of the different conformers. Several approaches have been proposed to reduce the number of variables, such as, for example, maximum entropy,<sup>20</sup> additive potential,<sup>21</sup> inertial frame,<sup>22</sup> and Monte Carlo methods.<sup>23</sup> However, given the complexity of the systems investigated here and the limited number of experimental data available, none of these methods can be applied without severe assumptions and/or simplifications. Therefore, we did not

attempt to obtain information on the conformational distribution but explored the compatibility of our data with conformations differing in the values of the dihedral angles  $\phi_1$  ( $\text{C}_{7'}\text{--O--C}_1\text{--C}_2$ ) and  $\phi_2$  ( $\text{C}_{7'}\text{--O--C}_1\text{--C}_3$ ), thus making the bold assumption that a single conformer dominates (see Figure 3). In fact, the flexibility of the central three ring fragment can be safely limited to the torsional rotation around the  $\text{C}_{\text{ar}}\text{--O}$  bonds since the benzoate groups can be considered planar due to strong conjugation effects<sup>24</sup> and the  $\text{C}_3\text{--O--C}_{7'}\text{--C}_{1'}$  and  $\text{C}_1\text{--O--C}_{7'}\text{--C}_{1'}$  dihedral angles have limited degrees of freedom, with values around  $180^\circ$ , due to a high rotational barrier.<sup>10</sup> The  $\phi_1$  and  $\phi_2$  angles define the positions of the carboxylic  $\text{sp}^2$  oxygen atoms adjacent to the central ring as explained in the caption of Figure 4. When the two CO groups are on opposite sides with respect to the central ring plane the conformers are defined as type 1, whereas when they are on the same side they are of type 2. Torsional angles relative to fragments further along the lateral wings were not investigated since our data are relative to deuteria on the central and lateral  $\alpha$  and  $\beta$  rings only.

For each molecule in each solvent, quadrupolar and dipolar splittings collected at different temperatures were globally analyzed by means of a nonlinear least-squares fitting procedure as a function of geometrical and orientational parameters (i.e.,  $\phi_1$  and  $\phi_2$  and the elements of the Saupe order matrix with respect to the  $(X,Y,Z)$  molecular frame located as shown in Figure 3). In the fitting procedure, for CIPbis11BB and CIPbisB,  $\phi_1$  and  $\phi_2$  were varied in steps of  $10^\circ$  in the ranges of  $0^\circ$ – $180^\circ$  and  $0^\circ$ – $350^\circ$ , respectively, while, for Pbis11BB and PbisB,  $\phi_1$  and  $\phi_2$  were varied in steps of  $5^\circ$  in the range of  $0^\circ$ – $180^\circ$  with either  $\phi_1 = \phi_2$  or  $\phi_1 = -\phi_2$ . For each conformer, characterized by a  $\phi_1, \phi_2$  pair, the optimized geometry obtained from DFT calculations was used. Since no direct information on the sign of the quadrupolar and dipolar couplings can be obtained from the spectra, in the data analysis all physically acceptable combinations of splitting signs were examined. Quadrupolar and dipolar splittings relative to deuteria on the same  $\alpha$  (or  $\beta$ ) ring were calculated as an average of  $D_4$  and  $D_5$  (or  $D_6$  and  $D_7$ ) splittings, given the observed spectral equivalence. Moreover, for the chlorinated compounds, due to the uncertainty in the assignment of the inner doublets to  $D_{4,5}$  or  $D_{6,7}$  deuteria, we performed the fitting for both attributions.

At each temperature, the independent elements of the Saupe order matrix for each conformer were determined (i.e.,  $S_{ZZ}$ ,  $S_{XZ}$ ,  $S_{YZ}$ ,  $S_{XX} - S_{YY}$ , and  $S_{XY}$  for the chlorinated molecules and for the non-chlorinated ones,  $S_{ZZ}$ ,  $S_{XX} - S_{YY}$ , together with  $S_{XY}$  for conformers of type 2 or  $S_{XZ}$  for conformers of type 1, as required on the basis of molecular symmetry).<sup>25</sup>

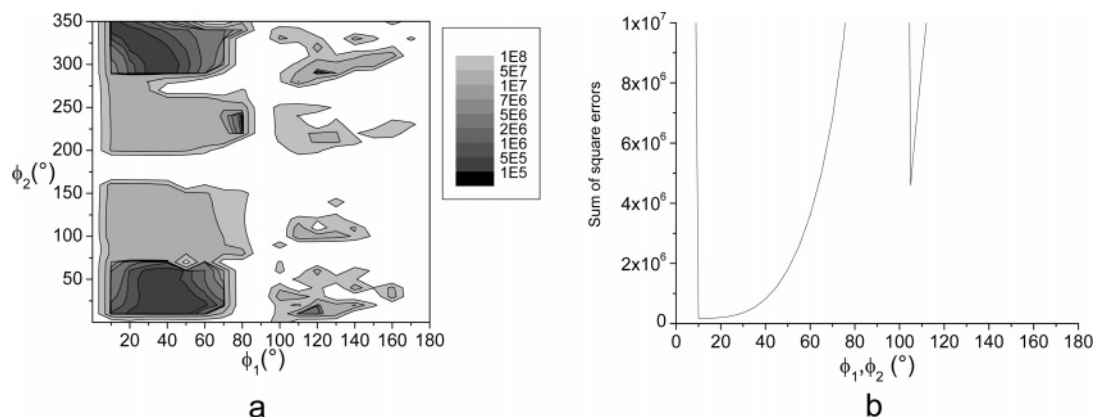


**Figure 5.** Sum of the squared deviations of the experimental values from the calculated splittings as a function of (a)  $\phi_1$  and  $\phi_2$  for CIPbis11BB in Phase IV and (b)  $\phi_1 (= \phi_2)$  for Pbis11BB in Phase IV.

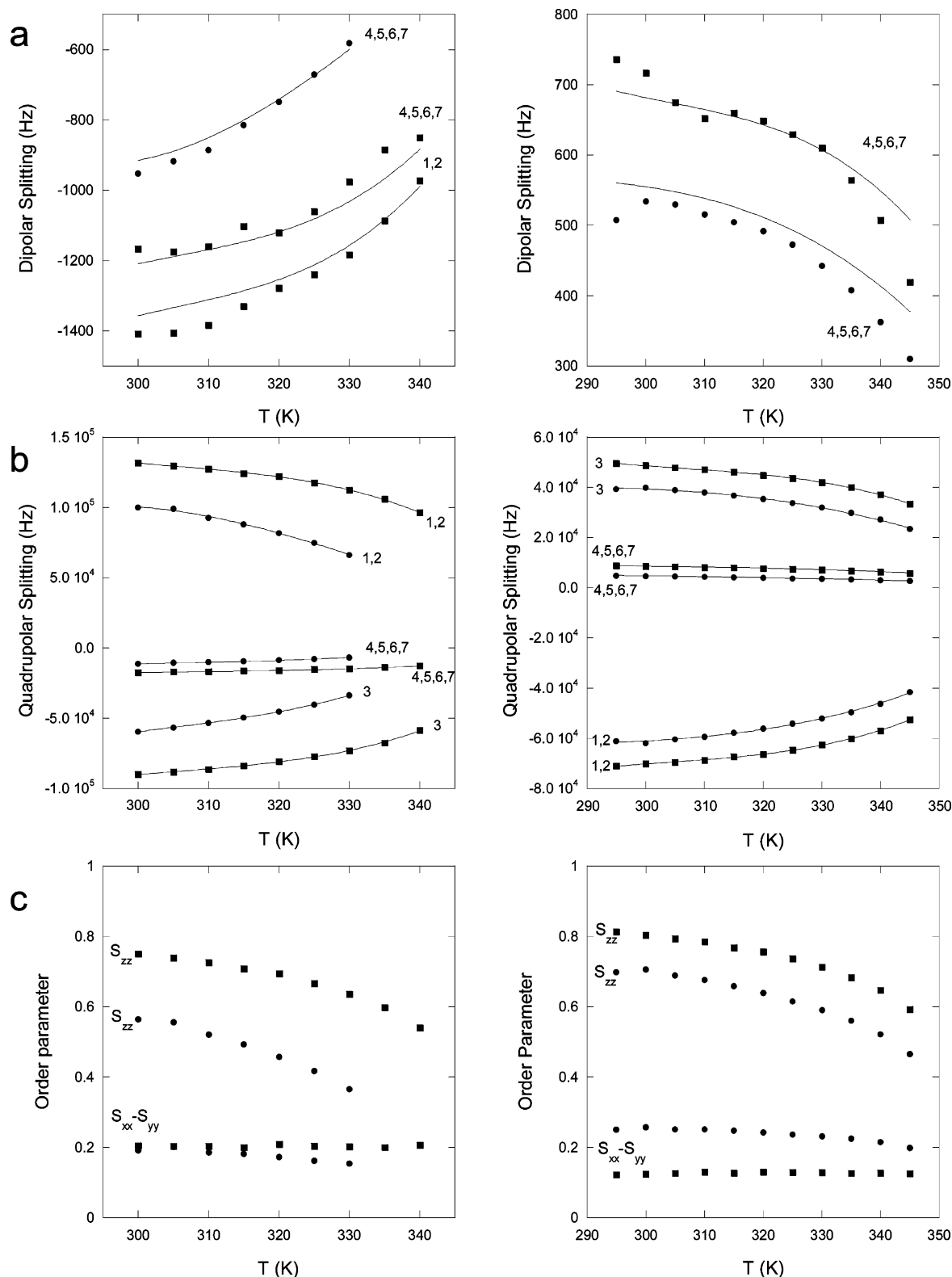


**Figure 6.** Experimental (symbols) and calculated (lines) of dipolar (a) and quadrupolar (b) splittings and calculated order parameters (c) of the banana-shaped mesogen Pbis11BB and the corresponding three ring molecule PbisB in Phase IV (left column) and ZLI1167 (right column). Circles and squares refer to three and five ring molecules, respectively. Calculations refer to the best-fitting conformers (i.e.,  $\phi_1 = \phi_2 = 25^\circ$  and  $40^\circ$  for Pbis11BB in Phase IV and ZLI1167, respectively, and  $\phi_1 = \phi_2 = 45^\circ$  for PbisB both in Phase IV and ZLI1167, respectively).

In all cases, also considering the possible combinations of splitting signs and assignments, a limited number of conformations gave a satisfactory reproduction of all the experimental data, the sum of the squared deviations as a function of  $\phi_1$  and  $\phi_2$  showing sharp minima. For CIPbis11BB, the experimental data are well-reproduced when the couples  $(\phi_1, \phi_2)$  assume values

in the regions  $(10^\circ-70^\circ, 300^\circ-350^\circ)$  and  $(10^\circ-70^\circ, 10^\circ-70^\circ)$ , as exemplified in Figure 5a for CIPbis11BB in Phase IV. For CIPbisB, two additional regions, namely,  $(110^\circ-140^\circ, 290^\circ-300^\circ)$  and  $(150^\circ-170^\circ, 20^\circ-50^\circ)$ , showed acceptable minima. For the non-chlorinated molecules, the best-fittings were always obtained with  $\phi_1 = \phi_2$  and  $\phi_1 = -\phi_2$  with values in the range

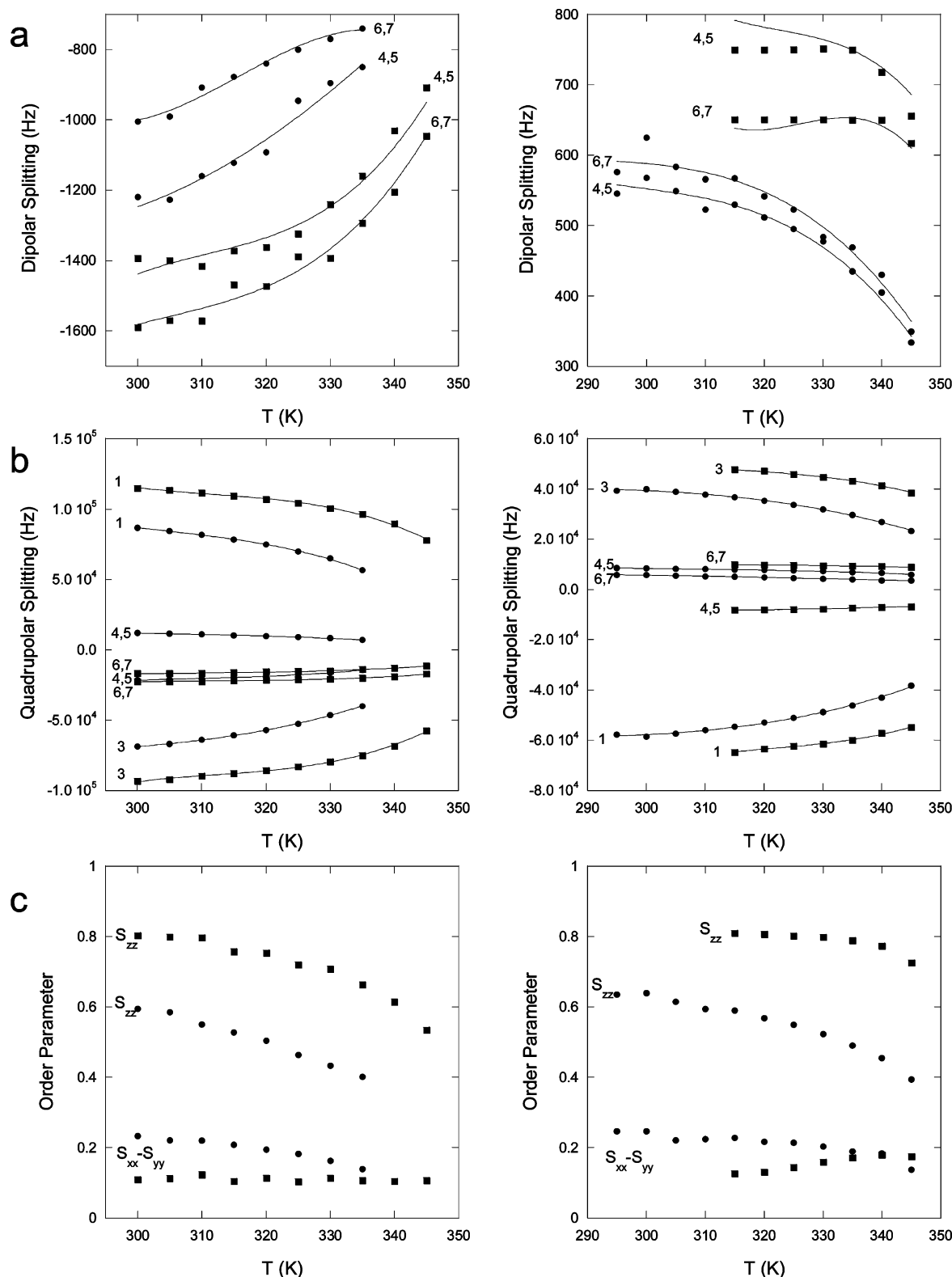


**Figure 7.** Experimental (symbols) and calculated (lines) of dipolar (a) and quadrupolar (b) splittings and calculated order parameters (c) of the banana-shaped mesogen CIPbis11BB and the corresponding three ring molecule CIPbisB in Phase IV (left column) and ZLI1167 (right column). Circles and squares refer to three and five ring molecules, respectively. Calculations refer to the best-fitting conformers (i.e.,  $(\phi_1, \phi_2) = (30^\circ, 320^\circ)$  and  $(30^\circ, 300^\circ)$  for CIPbis11BB in Phase IV and ZLI1167, respectively, and  $(\phi_1, \phi_2) = (50^\circ, 330^\circ)$  and  $(20^\circ, 290^\circ)$  for CIPbisB in Phase IV and ZLI1167, respectively).

of  $10^\circ$ – $60^\circ$ ; the example of conformers with  $\phi_1 = \phi_2$  is shown in Figure 5b for Pbis11BB in Phase IV.

For all the conformations yielding acceptable errors, diagonalization of the Saupe matrix gave the principal order parameters  $S_{zz}$ ,  $S_{xx}$ ,  $S_{yy}$  and the orientation of the order Principal Axis System  $(x, y, z)$  in the molecular fixed frame  $(X, Y, Z)$ .

Conformations giving physically unacceptable values of these parameters were discarded. After this screening, the  $(\phi_1, \phi_2)$  regions allowed for CIPbis11BB were restricted to  $(30^\circ, 300^\circ$ – $320^\circ)$  for type 1 conformers and  $(25^\circ$ – $50^\circ, 20^\circ$ – $25^\circ)$  for type 2 conformers, while the regions  $(20^\circ$ – $50^\circ, 290^\circ$ – $340^\circ)$  and  $(10^\circ$ – $50^\circ, 10^\circ$ – $50^\circ)$  were acceptable for CIPbisB. A  $\phi_2$  angle

**TABLE 1: Dihedral Angles  $\phi_1$  and  $\phi_2$  of the Best-Fitting Conformers and Relative Euler Angles ( $\alpha, \beta, \gamma$ ) Defining the Order Principal Axes System with Respect to the Molecule Fixed Frame<sup>a</sup>**

molecule	solvent	$\phi_1$	$\phi_2$	$\alpha$	$\beta$	$\gamma$	bending angle
Pbis11BB	ZLI1167	35	325	90	90	90	141
		40	40	-15	0	0	136
	Phase IV	35	325	90	90	90	141
		25	25	28	0	0	145
CIPbis11BB	ZLI1167	30	300	12	-17	-6	137
		25	25	-68	1	86	149
	Phase IV	30	320	69	3	-65	140
		50	20	-38	13	36	141
PbisB	ZLI1167	30	330	90	90	90	142
		45	45	-28	0	0	131
	Phase IV	30	330	90	90	90	142
		45	45	-25	0	0	131
CIPbisB	ZLI1167	20	290	61	-8	-65	137
		45	40	24	-12	-51	134
	Phase IV	50	330	10	-21	21	138
		30	20	32	-8	-35	142

<sup>a</sup> In the last column, the bending angle calculated for each conformer is also reported. The values of all the angles are given in degrees.

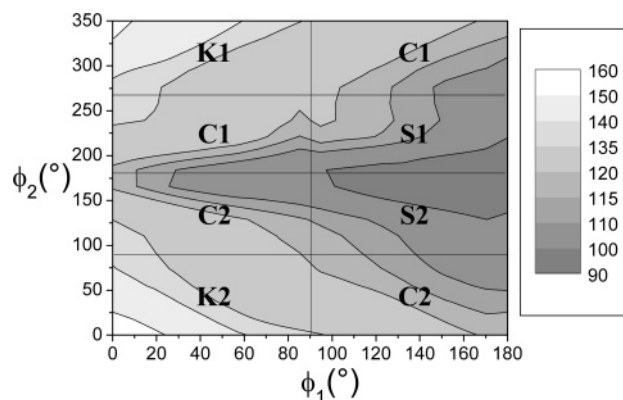
of  $10^\circ$ – $50^\circ$  or  $290^\circ$ – $340^\circ$  is also expected on the basis of DFT calculations<sup>13</sup> ascribable to the strong steric repulsion between the chlorine atom and the neighboring carboxylic  $sp^2$  oxygen atom. On the contrary, a  $\phi_1$  value of  $10^\circ$ – $50^\circ$  does not correspond to the minimum energy conformation found by this method.<sup>13</sup> On the other hand, the most stable conformation found for CIPbis11BB using the semiempirical MOPAC/AM1 method<sup>9</sup> has a K-type conformation (see Figure 4), as found by us.

For the non-chlorinated molecules, conformations with  $\phi_1 = \phi_2$  and  $\phi_1 = -\phi_2$ , with values in the range of  $25^\circ$ – $45^\circ$ , remained with only small differences in the two solvents in the case of Pbis11BB. The latter corresponds to the low DFT energy minimum conformation K1 of ref 13, whereas the former corresponds to the relatively high DFT energy minimum conformation K2<sup>13</sup> but coincides with the most stable conformation obtained by MOPAC/AM1.<sup>9</sup>

It should be noticed that the conformers selected by our procedure can be considered substantially independent of the detailed molecular local geometries; in fact, the best-fitting  $\phi_1, \phi_2$  couples obtained using relaxed geometries are not significantly different from those obtained from frozen local geometries corresponding to DFT energy minima by varying  $\phi_1$  and  $\phi_2$ .

The splittings of the best-fitting conformers obtained for Pbis11BB and PbisB and for CIPbis11BB and CIPbisB are shown in Figures 6a,b and 7a,b, respectively, together with the experimental ones; the relative order parameters are reported in Figures 6c and 7c, respectively. The values of the principal order parameter  $S_{zz}$  are in the range of 0.4–0.7 for the three ring molecules and up to 0.8 for the five ring ones, with higher values in ZLI1167. The biaxiality  $S_{xx} - S_{yy}$  is non-negligible in all cases, as commonly observed for solutes with symmetry axis  $C_n$  with  $n < 3$  in nematic solvents.<sup>26</sup> Depending on the solute and on the solvent, a slight temperature dependence of the biaxiality is observed. In general, the three ring solutes are characterized by a higher biaxiality with respect to the corresponding five ring ones, as expected given the sensibly shorter end chains. Moreover, the solvent seems to differently affect the biaxiality of the chlorinated and non-chlorinated molecules.

The orientation of the PAS systems ( $x, y, z$ ) with respect to the molecule fixed frames ( $X, Y, Z$ ) for the best-fitting conformers is given by the Euler angles reported in Table 1. For the non-chlorinated molecules, where the  $z$  and  $Z$  axes have been assumed coincident on the basis of symmetry, a small rotation

**Figure 8.** Bending angle (degrees) and conformations as a function of  $\phi_1$  and  $\phi_2$  for CIPbisB.

of the  $x, y$  axes is observed for conformations of type 2, while  $z$  coincides with  $Y$  and  $y$  with  $Z$  for the conformations of type 1. In the case of the chlorinated molecules, the two axes systems are quite close, the largest difference being observed for CIPbisB in Phase IV, which is characterized by  $\phi_1 = 50^\circ$  and  $\phi_2 = 330^\circ$ .

The bending angles found for the best-fitting conformers, defined here as the angle between the  $\alpha$  and  $\beta$  para axes, are reported in Table 1. As can be seen, these angles are rather similar for the chlorinated and non-chlorinated molecules and cover a quite limited range, falling in the high side of the  $110^\circ$ – $140^\circ$  interval considered as optimal for the formation of the B phases.<sup>1,3</sup> Clearly, these angles strongly depend on  $\phi_1, \phi_2$ , which, in turn, affect the local geometry; in particular, the angles  $C_2-C_1-O$  and  $C_2-C_3-O$  in the relaxed geometries are found to vary by more than  $10^\circ$  with  $\phi_1$  and  $\phi_2$ , while smaller but significant changes are determined for  $C_1-O-C_7$  and  $C_3-O-C_7$ . An example of this dependence is shown in Figure 8 for CIPbisB, where the bending angle spans a range of about  $70^\circ$  around  $122^\circ$ , with higher and lower values for the K and S conformers, respectively. It is interesting to note that for both type 1 and 2 conformers, this angle decreases with increasing  $\phi_1$ . Moreover, it can be observed that bending angles within the  $110^\circ$ – $140^\circ$  range are compatible, at least for the case here shown, with all types of conformations.

The similarity in bending angle obtained for the different molecules is therefore to be ascribed to the similar best-fitting conformers obtained, the small differences being due to different local geometries. The value of  $\sim 140^\circ$  here obtained for CIPbis11BB is similar to that found from  $^2H$  and  $^{13}C$  measurements in its nematic phase ( $144.3^\circ$  and  $136.6^\circ$ , respectively).<sup>11</sup> In addition, large bending angles (between  $141^\circ$  and  $154^\circ$ , calculated according to our definition from the atomic coordinates) were obtained from X-ray measurements on 1,3-phenylene bis[4-(4- $n$ -alkoxy-phenyliminomethyl)benzoates] with two chlorine atoms on the central ring in positions 4 and 6.<sup>7,8</sup>

Finally, it must be pointed out that, for all the molecules investigated, acceptable solutions corresponding to both type K1 and K2 conformations are obtained; with the data available, it is not possible to exclude one of the two, also considering that both types of conformations have been observed in similar systems in the crystalline phase.<sup>7,8</sup>

## Conclusions

$^2H$  NMR data collected at various temperatures in two nematic solvents on two banana-shaped mesogens, CIPbis11BB and Pbis11BB, differing for a chlorine atom on the central ring, were analyzed to obtain information on the conformation. The data are compatible only with K type conformations, differently



from what is expected from theoretical calculations but in agreement with X-ray experiments in the crystalline phase. On the other hand, the data do not give unequivocal evidence on the relative position of the two CO groups with respect to the plane of the central ring. The  $^2\text{H}$  NMR measurements carried out on the corresponding three ring molecules PbisB and CIPbisB did not detect significant differences with respect to the five ring molecules, suggesting that these systems can be safely used as models for the conformational equilibria of the mesogens themselves.

The results obtained do not allow for remarkable differences in the preferred conformation and bending angle for CIPbis11BB and Pbis11BB, although they show different mesomorphic behavior, thus suggesting that the hypothesis of a strong relationship between bending angle, determined by chlorine substitution on the central phenyl ring, and mesomorphic behavior is objectionable.<sup>27</sup> Other molecular properties, such as polarity, which have been considered in theoretical studies,<sup>10</sup> probably should be taken into account in predicting the mesomorphic behavior of banana-shaped mesogens.

**Acknowledgment.** The authors are thankful to A. Ferretti (IPCF-CNR) for allowing them to perform preliminary DFT calculations. The authors thank the Hungarian Research Fund OTKA K61075, the COST program D35 WG13-05, and the CNR-MTA joint project 2004–2006 on novel polymers made from banana-shaped monomers.

**Supporting Information Available:** Analytical and spectral characterization data of synthesized compounds. This material is available free of charge via the Internet at <http://pubs.acs.org>.

## References and Notes

- (1) Pelzl, G.; Diele, S.; Weissflog, W. *Adv. Mater.* **1999**, *11*, 707–724.
- (2) Ros, M. B.; Serrano, J. L.; De La Fuente, M. R.; Folcia, C. L. *J. Mater. Chem.* **2005**, *15*, 5093–5098.
- (3) Weissflog, W.; Nádasi, H.; Dunemann, U.; Pelzl, G.; Diele, S.; Eremin, A.; Kresse, H. *J. Mater. Chem.* **2001**, *11*, 2748–2758.
- (4) Bedel, J. P.; Rouillon, J. C.; Marcerou, J. P.; Laguerre, M.; Nguyen, H. T.; Achard, M. F. *J. Mater. Chem.* **2002**, *12*, 2214–2220.
- (5) Dunemann, U.; Schröder, M. W.; Reddy, R. A.; Pelzl, G.; Diele, S.; Weissflog, W. *J. Mater. Chem.* **2005**, *15*, 4051–4061.
- (6) Weissflog, W.; Naumann, G.; Kosata, B.; Schröder, M. W.; Eremin, A.; Diele, S.; Vakhovskaya, Z.; Kresse, H.; Friedemann, R.; Krishnan, S. A. R.; Pelzl, G. *J. Mater. Chem.* **2005**, *15*, 4328–4337.
- (7) Weissflog, W.; Lischka, C.; Diele, S.; Pelzl, G.; Wirth, I.; Grande, S.; Kresse, H.; Schmalfuss, H.; Hartung, H.; Stettler, A. *Mol. Cryst. Liq. Cryst.* **1999**, *333*, 203–235.
- (8) Hartung, H.; Stettler, A.; Weissflog, W. *J. Mol. Struct.* **2000**, *526*, 31–40.
- (9) Fodor-Csorba, K.; Vajda, A.; Galli, G.; Jákli, A.; Demus, D.; Holly, S.; Gács-Baitz, E. *Macromol. Chem. Phys.* **2002**, *203*, 1556–1563.
- (10) Ananda Rama Krishnan, S.; Weissflog, W.; Friedemann, R. *Liq. Cryst.* **2005**, *32*, 847–856.
- (11) Dong, R. Y.; Fodor Csorba, K.; Xu, J.; Domenici, V.; Prampolini, G.; Veracini, C. A. *J. Phys. Chem. B* **2004**, *108*, 7694–7701.
- (12) Xu, J.; Dong, R. Y.; Domenici, V.; Fodor Csorba, K.; Veracini, C. A. *J. Phys. Chem. B* **2006**, *110*, 9434–9441.
- (13) Cacelli, I.; Prampolini, G. *Chem. Phys.* **2005**, *314*, 283–290.
- (14) Imase, T.; Kawauchi, S.; Watanabe, J. *J. Mol. Struct.* **2001**, *560*, 275–281.
- (15) Domenici, V.; Madsen, L. A.; Choi, E. J.; Samulski, E. T.; Veracini, C. A. *Chem. Phys. Lett.* **2005**, *402*, 318–323.
- (16) Catalano, D.; Chiellini, E.; Chiezz, L.; Fodor-Csorba, K.; Galli, G.; Gács-Baitz, E.; Holly, S.; Veracini, C. A. *Mol. Cryst. Liq. Cryst.* **1999**, *336*, 111–122.
- (17) Galli, G.; Ragnoli, M.; Chiellini, E.; Komitov, L.; Andersson, G. *Ferroelectrics* **2002**, *276*, 37–44.
- (18) Frisch, M. J.; Trucks, G. W.; Schlegel, H. B.; Scuseria, G. E.; Robb, M. A.; Cheeseman, J. R.; Montgomery, J. A., Jr.; Vreven, T.; Kudin, K. N.; Burant, J. C.; Millam, J. M.; Iyengar, S. S.; Tomasi, J.; Barone, V.; Mennucci, B.; Cossi, M.; Scalmani, G.; Rega, N.; Petersson, G. A.; Nakatsuji, H.; Hada, M.; Ehara, M.; Toyota, K.; Fukuda, R.; Hasegawa, J.; Ishida, M.; Nakajima, T.; Honda, Y.; Kitao, O.; Nakai, H.; Klene, M.; Li, X.; Knox, J. E.; Hratchian, H. P.; Cross, J. B.; Bakken, V.; Adamo, C.; Jaramillo, J.; Gomperts, R.; Stratmann, R. E.; Yazyev, O.; Austin, A. J.; Cammi, R.; Pomelli, C.; Ochterski, J. W.; Ayala, P. Y.; Morokuma, K.; Voth, G. A.; Salvador, P.; Dannenberg, J. J.; Zakrzewski, V. G.; Dapprich, S.; Daniels, A. D.; Strain, M. C.; Farkas, O.; Malick, D. K.; Rabuck, A. D.; Raghavachari, K.; Foresman, J. B.; Ortiz, J. V.; Cui, Q.; Baboul, A. G.; Clifford, S.; Cioslowski, J.; Stefanov, B. B.; Liu, G.; Liashenko, A.; Piskorz, P.; Komaromi, I.; Martin, R. L.; Fox, D. J.; Keith, T.; Al-Laham, M. A.; Peng, C. Y.; Nanayakkara, A.; Challacombe, M.; Gill, P. M. W.; Johnson, B.; Chen, W.; Wong, M. W.; Gonzalez, C.; Pople, J. A. *Gaussian 03*, revision A.1; Gaussian, Inc.: Pittsburgh, PA, 2004.
- (19) (a) Becke, A. D. *J. Chem. Phys.* **1993**, *98*, 5648–5652. (b) Lee, C.; Yang, W.; Parr, R. G. *Phys. Rev. B* **1988**, *37*, 785–789.
- (20) Zannoni, C. In *Nuclear Magnetic Resonance of Liquid Crystals*; Emsley, J. W., Ed.; Reidel: Dordrecht, The Netherlands, 1985; Vol. 141, Ch. 1, p 11.
- (21) Emsley, J. W.; Luckhurst, G. R.; Stockley, C. P. *Proc. R. Soc. London, Ser. A* **1982**, *381*, 117–138.
- (22) Samulski, E. T.; Dong, R. Y. *J. Chem. Phys.* **1982**, *77*, 5090–5096.
- (23) Zannoni, C. In *The Molecular Physics of Liquid Crystals*; Luckhurst, G. R.; Gray, G. W., Eds.; Academic Press: New York, 1979.
- (24) Wrzalik, R.; Merkel, K.; Kocot, A. *J. Mol. Model* **2003**, *9*, 248–258.
- (25) Klyne, W.; Prelog, V. *Experientia* **1960**, *16*, 521–523.
- (26) Emsley, J. N.; Lindon, J. C. *NMR Spectroscopy Using Liquid Crystal Solvents*; Pergamon Press: Oxford, 1975.
- (27) Weissflog, W.; Sokolowski, S.; Dehne, H.; Das, B.; Grande, S.; Schröder, M. W.; Eremin, A.; Diele, S.; Pelzl, G.; Kresse, H. *Liq. Cryst.* **2004**, *31*, 923–933.